AGU PUBLICATIONS

Water Resources Research

RESEARCH ARTICLE

10.1002/2015WR018225

Key Points:
- Hyporheic transport in constrained valleys is controlled by geologic setting
- Hyporheic transport near large in-stream features is not variable with discharge
- Transport in broad riparian zones is controlled by dynamic hydrologic forcing

Supporting Information:
- Supporting Information S1
- Movie S1
- Movie S2
- Movie S3

Correspondence to:
A. S. Ward,
adamward@indiana.edu

Citation:
Ward, A. S., N. M. Schmadel, S. M. Wondzell, C. Harman, M. N. Gooseff, and K. Singha (2016), Hydrogeomorphic controls on hyporheic and riparian transport in two headwater mountain streams during base flow recession, *Water Resour. Res.*, *52*, doi:10.1002/2015WR018225.

Received 11 OCT 2015
Accepted 8 FEB 2016
Accepted article online 12 FEB 2016

Hydrogeomorphic controls on hyporheic and riparian transport in two headwater mountain streams during base flow recession

Adam S. Ward[1], Noah M. Schmadel[1], Steven M. Wondzell[2], Ciaran Harman[3], Michael N. Gooseff[4], and Kamini Singha[5]

[1]School of Public and Environmental Affairs, Indiana University, Bloomington, Indiana, USA, [2]Pacific Northwest Research Station, United States Department of Agriculture Forest Service, Corvallis, Oregon, USA, [3]Department of Geography and Environmental Engineering, Johns Hopkins University, Baltimore, Mary land, USA, [4]Institute of Arctic and Alpine Research and Department of Civil, Environmental, and Architectural Engineering, University of Colorado, Boulder, Colorado, USA, [5]Geology and Geological Engineering Department and Hydrologic Science and Engineering Program, Colorado School of Mines, Golden, Colorado, USA

Abstract Solute transport along riparian and hyporheic flow paths is broadly expected to respond to dynamic hydrologic forcing by streams, aquifers, and hillslopes. However, direct observation of these dynamic responses is lacking, as is the relative control of geologic setting as a control on responses to dynamic hydrologic forcing. We conducted a series of four stream solute tracer injections through base flow recession in each of two watersheds with contrasting valley morphology in the H.J. Andrews Experimental Forest, monitoring tracer concentrations in the stream and in a network of shallow riparian wells in each watershed. We found hyporheic mean arrival time, temporal variance, and fraction of stream water in the bedrock-constrained valley bottom and near large roughness elements in the wider valley bottom were not variable with discharge, suggesting minimal control by hydrologic forcing. Conversely, we observed increases in mean arrival time and temporal variance and decreasing fraction stream water with decreasing discharge near the hillslopes in the wider valley bottom. This may indicate changes in stream discharge and valley bottom hydrology control transport in less constrained locations. We detail five hydrogeomorphic responses to base flow recession to explain observed spatial and temporal patterns in the interactions between streams and their valley bottoms. Models able to account for the transition from geologically dominated processes in the near-stream subsurface to hydrologically dominated processes near the hillslope will be required to predict solute transport and fate in valley bottoms of headwater mountain streams.

1. Introduction

Beneficial functions of hyporheic and riparian zones primarily arise due to the extended contact time of water with the bioactive subsurface [e.g., *Findlay*, 1995]. Contact timescales are controlled by the interaction between dynamic hydrologic forcing and the geologic setting [*Ward et al*., 2012]. Studies of hyporheic transport often focus on steady state hydrologic conditions, and assume transport processes change systematically with discharge [e.g., *Covino et al*., 2011]. However, hydrologists are broadly recognizing that transport processes (e.g., advection and dispersion) are dynamic, responding to dynamic hydrologic forcing across a host of spatial scales [*Maloszewski and Zuber*, 1982; *McGuire and McDonnell*, 2006; *Ward et al*., 2013a; *Harman*, 2015]. Improved characterization of physical solute transport processes is required to accurately predict and quantify the beneficial functions associated with exchange of water across the stream-hyporheic-riparian-hillslope continuum. In this study, we seek to quantify hyporheic transport timescales and processes as a function of geologic constraints and dynamic hydrologic forcing through seasonal base flow recession in two headwater mountain streams with contrasting geologic setting.

Hyporheic exchange in headwater mountain streams is controlled by a combination of geologic and hydrologic factors [*Wondzell et al*., 2013]. Streambed morphology is tightly coupled to different mechanisms of exchange, including [after *Kaser et al*., 2009] turnover exchange when streambeds mobilize [e.g., *Elliott and Brooks*, 1997a; *Packman et al*., 2001], diffusion of turbulent momentum into the stream bed [e.g., *Packman and Bencala*, 2000], hydrostatic-driven exchange [e.g., *Harvey and Bencala*, 1993; *Kasahara and Wondzell*,

2003; *Gooseff et al*., 2006], and by hydrodynamic-driven pumping across beds and banks [*Elliott and Brooks*, 1997a,b; *Worman et al*., 2002]. Hydrogeologic setting includes heterogeneities ranging from parent lithology [e.g., *Valett et al*., 1996; *Payn*, 2009], lithologic unit structure in valley bottoms [*Vaux*, 1968; *Ryan et al*., 2004; *Ward et al*., 2011], hydraulic conductivity fields within individual lithologic units [*Packman and Salehin*, 2003; *Salehin et al*., 2004], and in grain bedding [*Sawyer and Cardenas*, 2009]. These grain-scale heterogeneities also generate interaction of mobile pore waters with less-mobile pore space along flow paths [*van Genuchten and Wierenga*, 1976]. Valley constraint has also been found to confine hyporheic zones and result in shorter exchange timescales [*D'Angelo et al*., 1993; *Stanford and Ward*, 1993; *Wright et al*., 2005; *Ward et al*., 2012].

Geologic controls interact with hydrologic controls to generate exchange fluxes and flow fields connecting streams and their valley bottoms (i.e., hyporheic-riparian-hillslope continuum). In headwater mountain streams, exchange is dominated by hydrostatic gradients near individual morphologic features [*Wondzell et al*., 2013], which can drive both vertical and lateral exchanges of water [*Lewandowski et al*., 2009]. At larger scales, hydraulic gradients link the stream, hyporheic zone, riparian zone, and hillslopes and are generally expected to control hyporheic extent and transit times [*Hynes*, 1983; *Meyer et al*., 1988; *Vervier et al*., 1992; *Hakenkamp et al*., 1993; *Palmer*, 1993; *White et al*., 1993]. However, this expected interaction has not been demonstrated in mountain streams. In particular, *Wondzell* [2006], *Ward et al*. [2012, 2014], *Wondzell and Swanson* [1996], and *Voltz et al*. [2013] found little change in hyporheic extent during base flow recession in headwater mountain streams with constrained valley bottoms. Still, these studies focus on hyporheic extent rather than transport along hyporheic flow paths.

Many field studies have relied solely upon in-stream solute tracer injections and in-stream monitoring to infer hyporheic responses to dynamic hydrologic forcing [*Payn*, 2009; *Covino et al*., 2011; *Ward et al*., 2013a,b]. The inherent window of detection and the convolution of both surface and subsurface dynamics into a single description of transient storage limit the utility of these methods to describe hyporheic processes [*Harvey et al*., 1996; *Choi et al*., 2000; *Drummond et al*., 2012]. Thus, studies without subsurface observations are likely to represent only the shortest and fastest hyporheic flow paths, and may be dominated by in-stream processes [*Wondzell*, 2011].

Studies that directly observe solute transport in the hyporheic zone gain insight by directly observing transport along hyporheic flow paths rather than inferring their behavior from an in-stream observation. Studies with direct subsurface observation have often overlooked dynamics of exchange, with few examples including repeated observations under different hydrologic conditions [*Gooseff et al*., 2004; *Wondzell*, 2006; *Voltz et al*., 2013]. Still, all such field studies interpret the combined impact of in-stream and hyporheic transport rather than isolating the hyporheic processes of interest. Combined interpretations of in-stream and hyporheic transport are common because the downwelling solute tracer time series, the starting point for hyporheic transport, integrates all upgradient transport processes. As such, hyporheic observations represent the convolution of all transport processes occurring between the injection location and downwelling location with those occurring along hyporheic flow paths. Assessment of hyporheic transport processes requires separation of in-stream transport, which is known to be highly sensitive to discharge [e.g., *Fischer*, 1979; *Jackson et al*., 2013], from hyporheic transport.

The objective of this study is to assess the change in hyporheic and riparian transit time distributions as a function of dynamic hydrologic forcing and the static geologic setting. We expect that direct observations of solute tracer in the hyporheic zone will demonstrate time-variable behavior through base flow recession due primarily to changes in transport along the stream. However, in cases where valley-bottom hydraulic gradients remain constant, we expect little change to the hyporheic transit time distribution since key controls such as hydraulic conductivity fields and down-valley gradients remain unchanged. Specifically, we seek to address the questions: (1) how do hyporheic transit times in a valley bottom vary with stream discharge through seasonal base flow recession?; and (2) how does the time-variability in hyporheic transit time distributions differ as a function of valley bottom location and bedrock constraint within and between geologic settings in neighboring catchments? To address these questions, we conducted a series of four solute tracer studies through the base flow recession period in two well-studied headwater mountain streams with contrasting valley bottom characteristics. Tracer concentrations were monitored in a network of shallow wells to directly assess hyporheic transport, and in the stream at several locations. The extensive surface and subsurface monitoring enabled separation of transport along hyporheic flow paths from in-stream transport. These data are used to contrast observed transport between two different valley bottom morphologies though base flow recession.

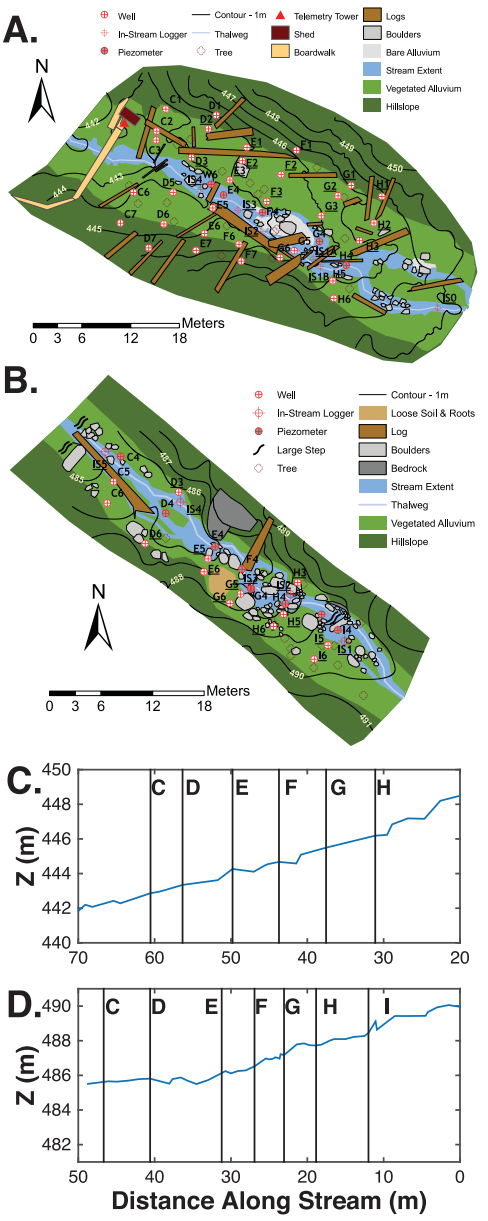

Figure 1. Study sites and instrumentation in watershed 1 (a; WS01) and watershed 3 (b; WS03) in the H.J. Andrews Experimental Forest, located in the western Cascade range in Oregon. Transects of wells and piezometers are labeled with a letter (downstream to upstream alphabetically) and number (increasing from North to South across the valley bottom). Stream centerline topography and the locations of transects for (c) WS01 and (d) WS03, with distance along the stream from an arbitrarily selected survey location on the *x* axis. Figures 1c and 1d are comparable to Figures 3 and 4 in *Wondzell* [2006]. Panels A and B reprinted with permission from *Voltz et al.* [2013].

2. Methods

2.1. Site Description and Hydrologic Monitoring

This study was conducted in watersheds 1 (WS01) and 3 (WS03), two headwater catchments in the H.J. Andrews Experimental Forest in the Cascade Mountains, Oregon, USA (Figure 1). The valley bottoms of the catchments are steep: about 11.9% and 13.8% down-valley gradients for WS01 and WS03, respectively. Both WS01 and WS03 have steep valley walls, with elevations ranging from 432 to 1018 m and 472 to 1077 m above mean sea level, respectively. Both catchments are underlain by shallow bedrock, with 1-2 m of highly porous soil above bedrock in the valley bottoms. Previous studies have documented a geometric mean saturated hydraulic conductivity of 1.7×10^{-5} m s^{-1} for valley bottom colluvium in WS01 [*Wondzell et al.*, 2009], and an average value of 7×10^{-5} m s^{-1} for all observations in WS01 and WS03 combined [*Kasahara and Wondzell*, 2003]. Both study reaches are located toward the lower elevations of their respective watersheds.

Both study catchments are gaged for discharge approximately 100 m downstream of the study reaches, with weirs calibrated and maintained by the U.S. Forest Service. Precipitation was monitored at the Primary Meteorological Station in the H.J. Andrews Experimental Forest. The study sites in WS01 and WS03 are highly instrumented with a network of shallow monitoring wells and piezometers constructed of polyvinyl chloride (PVC) screened with small holes and driven up to 1.7 m into the subsurface (<1 m in several locations). *Wondzell* [2006] provides additional detail on the construction of the monitoring well network. Discharge during our study ranged from 38.5 to 1.8 L s^{-1} in WS01, and from 37.5 to 4.3 L s^{-1} in WS03 (Figure 2a) through the period of base flow recession (June–August 2010). A 1.25 yr return interval storm occurred in mid-June 2010, prior to all tracer experiments in WS03, and between the first and second tracer experiments in WS01 [*Voltz et al.*, 2013].

There was little variation in valley bottom hydraulic gradients through the seasonal base flow recession during the study period (July–August 2010) [*Voltz et al.*, 2013]. In both WS01 and WS03, Voltz et al. [2013] report hydraulic gradients are generally dominated by down-valley direction (as opposed to cross-valley, where gradients would be predominantly toward the stream), and become increasingly down-valley dominant through the base flow recession period. Voltz et al. [2013] found only gradients near the hillslope on the south side of the stream in WS03 (between transects D and G, Figure 1) show periods of cross-valley dominance. Through our study period, water levels in the wells monitored by Voltz et al. [2013] fell by an average of 0.15 m in WS01 wells (range 0.04–0.24 m) and 0.10 m (range 0.01–0.28) in WS03. Stream water levels recorded at five sites in each study reach fell by an average of 0.09 m (range 0.04–0.17 m) in WS01 and 0.09 m (range 0.04–0.18 m) in WS03. The northern side-channels between transects F and G and

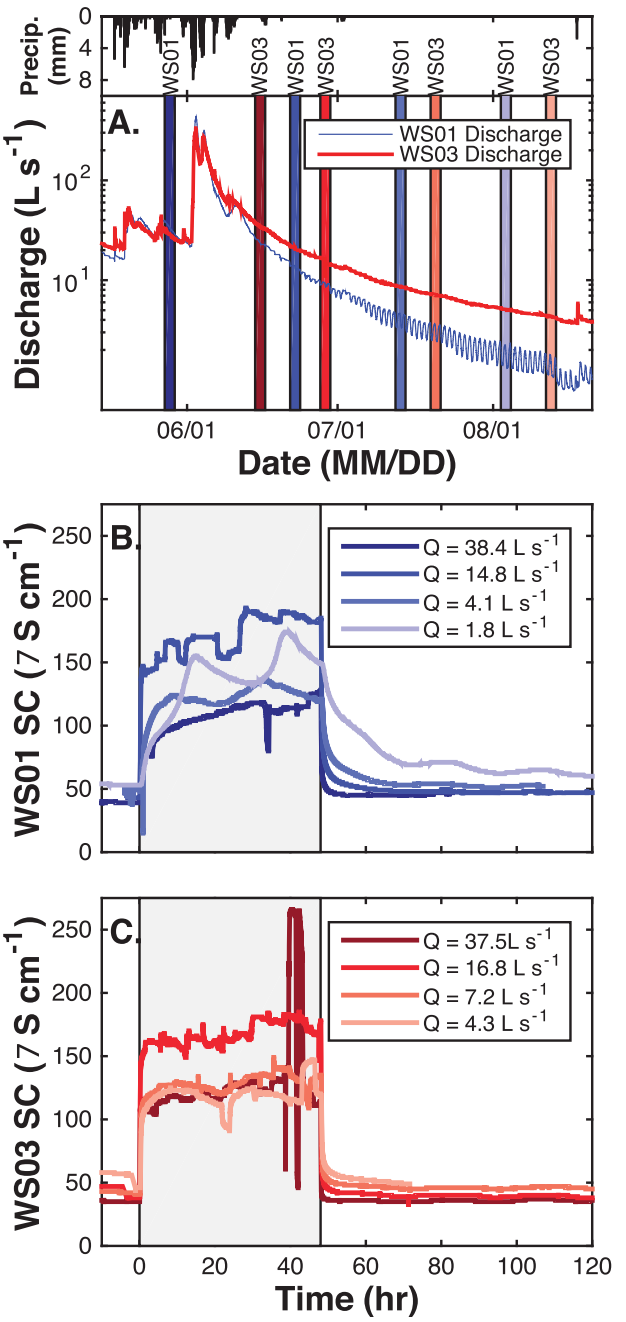

Figure 2. (a) Precipitation at the H.J. Andrews Primary Meteorological Station and discharge at the H.J. Andrews WS01 and WS03 stream gauges (each 50–100 m downstream of the study reach). The vertical bars show the constant rate 48 h injections conducted in each watershed for this study. In-stream solute tracer time series at the upstream end of the study reach for experiments in (b) WS01 and (c) WS03. Down-well time series are presented in supporting information Figure S1. Overall observations show increased late-time tailing during lower discharge conditions in both watersheds.

upstream of transect H in WS01 and the southern side-channels upstream of transect I and between transects C and D in WS03 were dry between the second and third injections; neither discharge nor stage observations were made in these channels. Further details of seasonal patterns are presented in Figures 5 and 6 of Voltz et al. [2013]. Additionally, vertical hydraulic gradients in and near the stream have been reported to remain constant through the study season in WS03 by *Ward et al* [2012]. *Wondzell* [2006] reported nearly constant vertical hydraulic gradients under high and low discharge conditions in WS03 and larger vertical hydraulic gradients from the stream to the subsurface during high discharge conditions in WS01.

The valley bottom of WS03 is highly constrained, averaging 8.5 m wide in the study reach (2.3 active channel widths) [*Wondzell*, 2006], with visible bedrock outcropping on both sides of the valley bottom. The lower portion of the study reach is a large gravel wedge held in place by a fallen tree, while the upper portion of the reach is characterized by boulders and porous alluvial deposits on the bedrock. *Kasahara and Wondzell* [2003] report 53.9% of elevation change in WS03 is due to steps and riffles (7.0 m of elevation changes per 100 m of stream length).The valley bottom of WS01 is less constrained than WS03, with an average width of 13.7 m through the study reach (3.5 active channel widths) [*Wondzell*, 2006]. *Kasahara and Wondzell* [2003] report steps and riffles contribute 51% of the change in elevation along the study reach in WS01 (representing about 6.6 m of elevation changes per 100 m of stream length). Additional physical descriptions of the H.J. Andrews Experimental Forest and the study sites are available in several other publications [*Dyrness*, 1969; *Swanson and James*, 1975; *Swanson and Jones*, 2002; *Wondzell*, 2006].

2.2. Solute Tracer Experiments and Monitoring in the Stream and Well Network

In each watershed, we conducted four 48 h constant rate injections of sodium chloride (NaCl), assumed to be a conservative tracer. Injections were conducted by pumping a concentrated NaCl solution directly into the stream at locations about 50 m upstream of each study reach, approximating the locations used by *Wondzell* [2006]. Pretracer specific conductance (SC) ranged from 39 to 53 μS cm^{-1} in WS01 and 35 to

46 μS cm^{-1} in WS03 (Figure 2). Injections were designed to achieve uniform plateau concentrations. In all monitoring, SC was used as a surrogate for tracer concentration.

In-stream SC and temperature were measured at several locations along each study reach at 30 s intervals with CS547A temperature and conductivity probes and recorded by a Campbell Scientific, Inc. (Logan, Utah, USA) data logger. These in-stream observations were made at a well-mixed location proximal to the injection (hereafter "upstream boundary"), and in the stream at multiple locations within the highly instrumented study reach. In the monitoring well network, SC was recorded by first purging at least one well volume and then using an EcoSense EC300 (YSI, Inc., Yellow Springs, Ohio, USA) or a model 107 Temperature/Level/Conductivity meter (Solinst, Inc., Georgetown, Ontario, Canada) deployed down the well and held in place until temperature and SC readings were stable. The wells were sampled sequentially, first moving along one transect and then moving downstream to the next transect. The stream SC was recorded with the same handheld loggers used in the wells each time the stream was crossed, with the exceptions of the first injection in WS01 for all transects, at well W6 for all injections in WS01, and at well F in WS03 for all injections. Sampling in the well network began prior to the injection to establish a baseline, and continued until wells returned to preinjection SC levels. Sampling frequency ranged from continuously cycling through the well network with each round of sampling taking about 40 min in WS01 and 25 min in WS03 to sampling at intervals of about 12 h during late-time tailing. This sampling routine established an observed solute tracer time series for the stream at each transect and for each observation well. We calculated the fraction of stream water present in each well as the ratio of the peak down-well concentration to peak in-stream concentration at each transect.

2.3. Temporal Metrics of Observed Solute Tracer Time Series

To compare in-stream and monitoring well tracer time series (hereafter breakthrough curve or BTC) across different discharge conditions and geologic settings, we first estimated summary metrics for each BTC. Prior to analysis, the high-resolution measurements in the stream were downsampled to match the temporal resolution of the monitoring well time series by interpolating the high temporal resolution in-stream time series to the times at which observations were made at the most nearby well. This downsampling was performed to provide an equal number of points collected at similar times such that in-stream and well time series could be compared. Higher-order temporal moments are known to amplify noise, particularly at late times, and this downsampling reduces the possibility of noise arising solely to different sampling frequencies.

In this time series analysis, we first calculated the time at which 99% of the total signal was recovered (t_{99}) by solving the following equation for t_{99}:

$$0.99 = \frac{\int_{t=0}^{t=t_{99}} tC(t)dt}{\int_{t=0}^{t=\infty} tC(t)dt} \tag{1}$$

where C is the observed tracer concentration. We truncated the observed time series at $t = t_{99}$ to minimize the subjective selection of the transition from signal to noise at late times [after *Mason et al.*, 2012; *Ward et al.*, 2013a,b, 2014]. We calculated a normalized time series for the tracer signal $c(t)$ as:

$$c(t) = \frac{C(t)}{\int_{t=0}^{t=t_{99}} C(t)dt} \tag{2}$$

Next, we calculated first-order temporal moments for the truncated time series as:

$$M_1 = \int_{t=0}^{t=t_{99}} tc(t)dt \tag{3}$$

In this case, M_1 represents the mean arrival time or centroid of the observed solute BTC. Finally, we calculated *nth*-order temporal moments about the centroid as:

$$\mu_n = \int_{t=0}^{t=t_{99}} (t - M_1)^n c(t)dt \tag{4}$$

The second central temporal moment is related to the temporal variance of the solute BTC. For transects where in-stream observations were not collected, we linearly interpolated temporal moments between observed sites.

2.4. Calculation of Transfer Functions for Hyporheic Flow Paths

The temporal moments of the transfer function, *g(t)*, allow isolation of the behavior of the transport system independently of the input signal of the stream concentration time series. The transfer function itself is related to the observed BTCs by the convolution integral for a system with linear behavior:

$$c(t) = \int_0^\infty g(\tau) c_{in}(t-\tau) d\tau \tag{5}$$

where c_{in} defines the input solute time series to the system. Rather than solving this integral, we isolated summary metrics of the transfer function signal using the change in observed temporal moments between two observations as:

$$M_1 = M_1^{output} - M_1^{input} \tag{6}$$

$$\mu_2 = \mu_2^{output} - \mu_2^{input} \tag{7}$$

where the superscripts "input" and "output" define the upstream and downstream observation sets, or inputs to and outputs from the flow path segment of interest. A similar deconvolution of transfer functions was recently conducted by *Ward et al*. [2014] to assess integrated transport along a stream and hyporheic flow paths in WS03.

In our study, observed temporal moments are available at three sets of locations: at the upstream boundary, in the stream channel at each transect, and in each monitoring well or piezometer. If flow is steady along a flow path, the temporal moments of the transfer function between any two points on the flow path can be estimated from the difference in the temporal moments of the transfer function between the points. Ideally, subtracting the temporal moment observed at the downwelling location from that observed at the monitoring well would complete isolation of the hyporheic transfer function. However, we lack the ability to identify the downwelling location(s) for the flow path(s) that intersect the screened section of any monitoring well. As such, we assume the temporal moment at the downwelling location is well-approximated by the temporal moment observed in the stream at each transect.

2.5. Estimation of Flow Path Lengths Associated With Temporal Transport Scales

To estimate the spatial scale of flow paths associated with the calculated transfer function metrics and assess the impact of assuming downwelling locations are at stream transects, we estimated subsurface velocities using Darcy's law:

$$V_{SUB} = \frac{K}{\eta} S \tag{8}$$

where V_{SUB} is the subsurface average linear velocity (m s^{-1}), K is hydraulic conductivity (m s^{-1}), η is porosity, and S is the hydraulic gradient (m m^{-1}). Using this estimated V_{SUB}, we calculated the length-scale associated with advection for the duration of M_1.

$$L = V_{SUB} M_1 \tag{9}$$

We assumed an average valley bottom gradient of 0.084 and 0.072 m m^{-1} for the study reaches in WS01 and WS03, respectively [*Voltz et al*., 2013]. This simplification approximates the hydraulic gradient in the valley bottom as equal to the topographic gradient along the stream centerline [*Wondzell*, 2011; *Ward et al*., 2013b]. We assumed a hydraulic conductivity of 7×10^{-5} m s^{-1} [*Kasahara and Wondzell*, 2003], and porosity of 50% (minimum value reported by *Dyrness* [1969]). By comparing magnitudes of changes along the stream to those along hyporheic flow paths, we can assess the validity of our assumption that the in-stream time series at each well transect is a good approximation of the downwelling time series.

2.6. Statistical Tests and Calculation of Trends

To test for transport differences between watersheds and discharges, we take the set of calculated metrics (M_1 and μ_2) for all wells and piezometers as a sample population. We use both parametric (one-way analysis of variance, ANOVA) and nonparametric (Kruskal-Wallis one-way analysis of variance by ranks) tests to quantify differences between watersheds and injections (i.e., different discharges). For this study, we use a 95% confidence level (i.e., $p < 0.05$) as our threshold for indication of significant differences between the

Table 1. Summary of Transport Metrics and Transfer Functions Observed in the System

		Upstream Boundary		In-Stream at Transect C		Transfer Function to Transect C		Along-Stream Distance Equal to:	
Catchment	Discharge ($L\ s^{-1}$)	M_1 (h)	μ_2 (h^2)	M_1 (h)	μ_2 (h^2)	M_1 (h)	μ_2 (h^2)	19.6[a] h in M_1 (m)	375.8[a] h^2 to μ_2 (m)
WS01	38	26.2	183	26.7	186.4	0.5	3.4	2940	8290
	15	25.3	191.3	29.1	340.7	3.8	149.5	387	189
	4.1	23.8	191.6	32.8	440.6	9	249.1	163	113
	1.8	23.5	178.2	54.3	2181.6	30.8	2003.5	48	14
	m[b]	0.073	−0.033	−0.51	−34.6	−0.59	−34.6	80.5	233.2
WS03	37	25.7	186.9	28.9	392.1	3.2	205.2	459	137
	17	24.6	190.8	26.1	218.2	1.5	27.5	980	1025
	7.2	25.3	221.4	32.7	738.9	7.4	517.5	199	54
	4.2	25.3	235.9	31.1	482.3	5.8	246.4	253	114
	m[b]	0.012	−1.4	−0.10	−6.7	−0.11	−5.3	7.9	2.5

[a]Interpolated or extrapolated based on the rate of change from the upstream location to transect C.
[b]Slope of linear regression with discharge.

population mean (ANOVA, *p*-values reported hereafter as p_{ANOVA}) and median (Kruskal-Wallis, *p*-values reported hereafter as p_{KW}) values. To assess trends with discharge at each monitoring location and trends with distance from the stream centerline, we fit a linear trend line to the relevant data points. We report the slope of the trend line, and consider the relationship significant (either positive or negative) if a slope of zero is not within the 95% confidence interval.

3. Results

3.1. Solute Tracer Observations in the Stream and Hyporheic Zone

In-stream plateaus at the upstream reach boundary ranged from about 110 to 190 μS cm^{-1} in WS01 and about 110 to 180 μS cm^{-1} in WS03 (Figures 2b and 2c). In-stream time series have increased late-time tailing under lower discharge conditions at well transect C in each watershed (i.e., the downstream boundary of the study reach; Table 1). Solute tracer time series for individual wells are provided in supporting information Figure S1. Time-lapse visualization of subsurface solute tracer concentrations is presented in supporting information Movie S1. A perfect constant-rate plateau with no spreading would have $M_1 = 24$ h and $\mu_2 = 192\ h^2$ at the upstream boundary. Based on observed data, we calculated input M_1 ranging from 23.8 to 26.2 h and input μ_2 ranging from 178.2 to 235.9 h^2. Deviations from the idealized inputs are due to increased influence of nonadvective processes between the injection and upstream boundary, as well as unsteady tracer mass loading rates (i.e., minor changes in pump speed and injectate concentration) and stream discharge over the 48 h injection period. Observed in-stream BTCs at transect C in both catchments exhibit expected trends of increased mean arrival time and temporal variance with decreasing discharge (Table 1). Trends are not monotonic with discharge, particularly within the WS03 observations. This may be caused by the temporary fluctuations in the injection rate and plateau concentration around hour 40 of the experiment for Injection 1 in WS03, which would shift M_1 to be artificially later than an experiment without this fluctuation. Still, the observed values are used because this was the measured input, and it has the potential to have impacted the monitoring well tracer time series. The best-fit linear slopes for M_1 and μ_2 with discharge are negative but not statistically significant. Transfer functions from the upstream boundary to transect C in each watershed, predominantly representing in-stream transport, show general trends of decreasing M_1 and μ_2 with increasing discharge through the season (Table 1). With slower advective transport in the channel (i.e., smaller M_1), there is more time for nonadvective processes (e.g., transient storage, dispersion) to act on the input signal and generate the observed trend in μ_2.

Next, we tested the assumption that in-stream temporal moments at the downwelling location of a hyporheic flow path, which remains unknown, can be approximated by those observed in the stream at the well transect. In our study, the mean and maximum M_1 values along hyporheic flow paths were 19.6 and 73.3 hr, respectively. Using the hyporheic potential estimates based on Darcy's law, these timescales correspond to estimated flow path length scales of 0.77 m and 2.88 m in WS01, and length scales of 0.83 m and 3.10 m in WS03. For comparison, a change in M_1 of 19.6 h due to transport along the advective channel ranges from

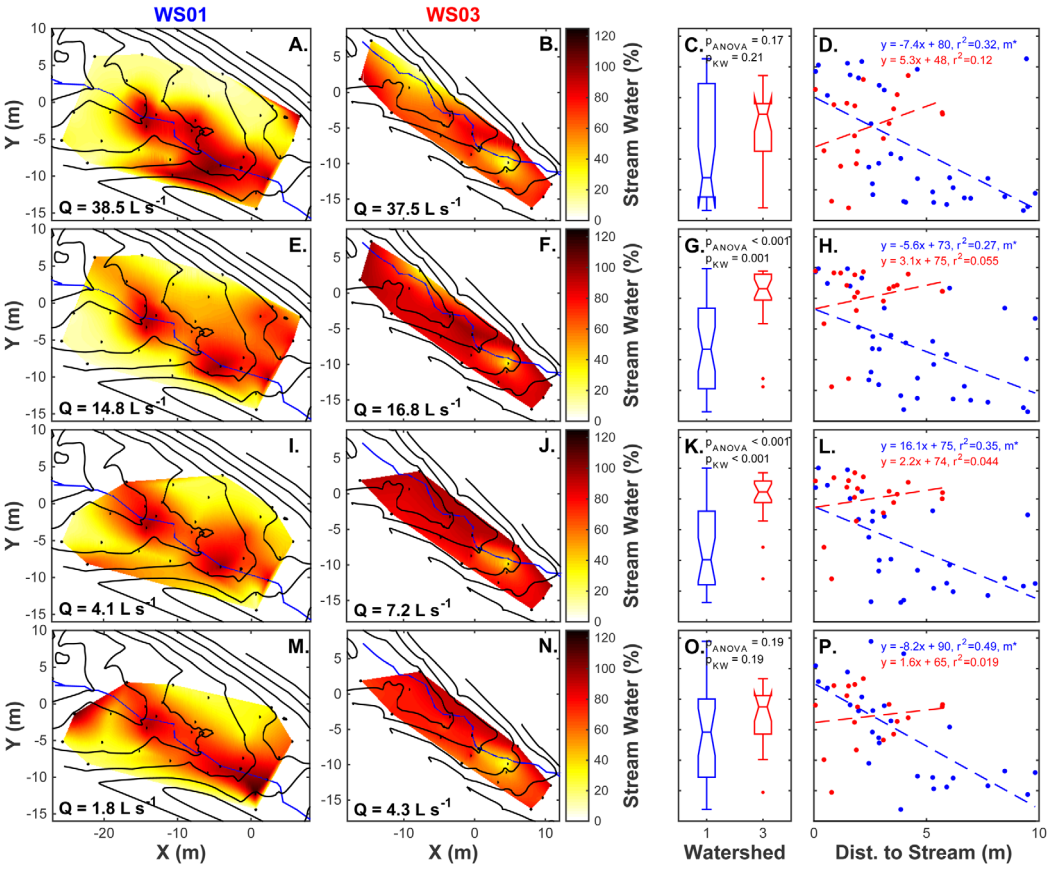

Figure 3. For all injections (sequentially from top to bottom), WS01 has a larger range of observed fractions of stream water, and WS03 always has a larger average fraction of stream water. The highly constrained WS03 exhibits no significant trends with distance from the stream centerline, while WS01 always exhibits significant trends of decreasing fraction of stream water with increasing distance from the stream centerline. Both one-way ANOVA and Kruskal-Wallis tests indicate significant differences in the population mean and median, respectively, for WS01 and WS03 during injections 2 and 3. Notation of m* indicates a slope that is significant (i.e., 0 is not within the 95% confidence interval for linear regression slope). Colorbars map to the *y* axis values on the two right-most columns, where the boxplots present the distribution of all observations for each flow condition. The scatter plots and best fit trend lines display trends in the peak fraction of stream water as a function of distance from the stream channel. Red and blue data sets on the figures represent WS01 and WS03, respectively. Figures 5–7 are displayed with a similar organization.

48 to 2940 m (Table 1), extrapolated from the observed changes in M_1 between the upstream boundary and Transect C observations in each study. In-stream distances to achieve a change equal to those observed along hyporheic flow paths are, on average, one to three orders of magnitude larger than the flow path length scale. This result suggests in-stream transport between the true downwelling location and the well transect are negligible compared to transformations along the hyporheic flow paths, justifying our assumption. Similarly, for μ_2, the average for all hyporheic transfer functions is 375.8 h^2, equivalent to the change expected from along-stream transport for 14–8290 m.

Peak tracer concentrations in wells lower than the peak in-stream concentration are an indicator of dilution of downwelling, tracer-labeled water. Sources of the unlabeled water may include a combination of down-valley subsurface flow bypassing the tracer injection and lateral inflows of water from the hillslopes to the valley bottom within the study reach. Additionally, dispersion along the flow path would reduce peak concentrations at the wells. We found 8 of the 195 total down-well solute tracer time series (about 4%) in which the fraction of stream water in a well was greater than 100% (in WS01, four for injection 1, one for injection 3, and two for injection 4, Figure 3). These eight observations range from 100.1 to 117.8% stream water (mean 105.2%, median 102.9%) and are attributed to error in field measurements or the presence of an unknown source, such as dissolution of substrate, along the flow path. There are several wells in WS01 where we consistently observed high concentrations of solute in all tracer injections (e.g., E4, E5, W6) suggesting these locations were persistent downwelling zones under all stream discharge conditions (Figure 3).

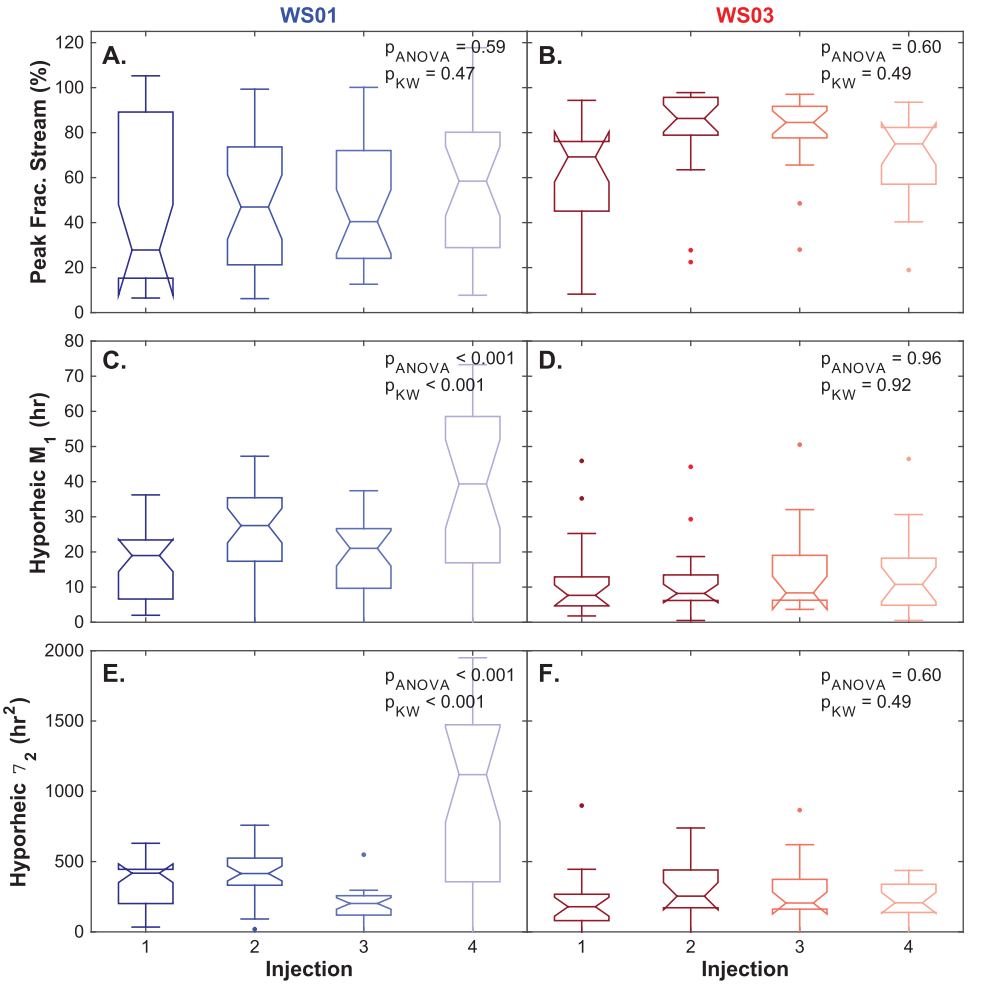

Figure 4. Box plots showing (a and b) the fraction of stream water at each monitoring well, (c and d) mean arrival time, M_1, at each well, and (e and f) temporal variance, μ_2 at each well for all injections in WS01 (left column) and WS03 (right column). Nonoverlapping notched regions indicate population medians are different at a 95% confidence level. *p*-Values for both the ANOVA and Kruskal-Wallis tests among all injections in a single watershed are shown. A *p*-value less than 0.05 indicates at least one injection is drawn from a population with a different mean (ANOVA) or median (Kruskal-Wallis).than at least one other. Through base flow recession, significant differences were observed in WS01 for hyporheic mean arrival time and temporal variance, but not fraction of stream water at a well. No significant differences through base flow recession were observed for WS03.

We also observed the opposite at well G3 in WS01 and H4 in WS03, where tracer concentration remained low throughout the duration of every tracer injection despite their location on the streambank (G3) and in the active channel (H4). Taking the monitoring wells as a sample of the population of hyporheic SC, the fraction of stream water in the wells is significantly higher in WS03 than in WS01 for injections 2 and 3 ($p_{ANOVA} < 0.001$ and $p_{KW} < 0.001$), but not for injections 1 or 4 ($p_{ANOVA} = 0.17$ and 0.19, $p_{KW} = 0.21$ and 0.21 for injections 1 and 4, respectively; Figure 3). In WS01, the fraction of stream water generally decreased with increasing distance from the stream centerline for all injections (statistically significant negative slopes for all injections, right most column in Figure 3). In WS03, the fraction of stream water generally increases with distance from the stream centerline for all injections, although the trend is not statistically significant in any cases.

Within-watershed comparisons were considered by comparing between injections in each watershed. In WS01, statistically significant differences in M_1 and μ_2 are present between some injections (Figures 4c, 4e, indicated by $p_{ANOVA} < 0.001$ and nonoverlapping notched regions of the boxplots). We found no statistical difference between injections for the estimated fraction of stream water in WS01 ($p_{ANOVA} = 0.59$ and $p_{KW} = 0.47$; Figure 4a). For WS03, the fraction of stream water, M_1, and μ_2 are not significantly between any pairs of injections (Figures 4b, 4d, and 4f).

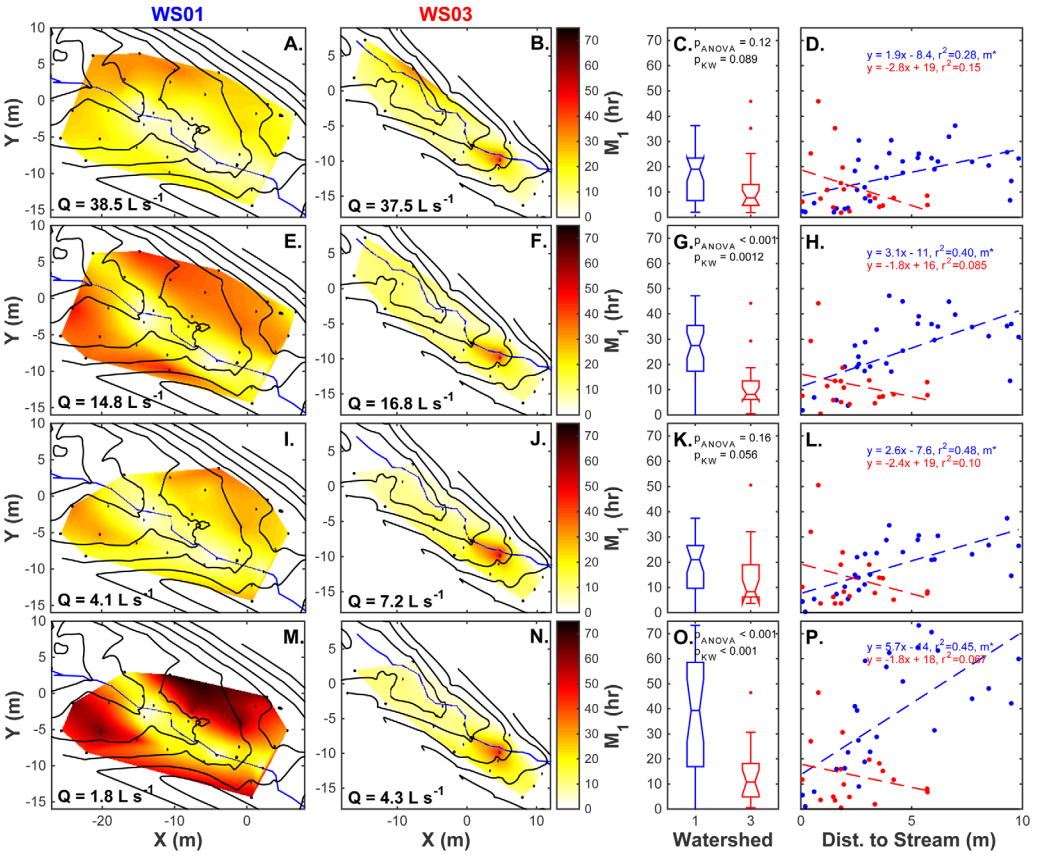

Figure 5. Mean arrival times for each well. For all injections, WS01 has a larger range and average value of observed transit times compared to WS03, likely owing to the wider valley bottom in WS01. In the wider WS01 valley bottom, mean transit time along a hyporheic flow path increases with distance from the stream centerline (trend is significant). For the more constrained WS03, a general trend of decreasing mean arrival time with increasing distance from the stream is observed in all cases, but the trend is not significant for any injections. Significant differences between WS01 and WS03 exist for mean arrival time for injections 2 and 4 based on both ANOVA and Kruskal-Wallis tests. Rapid arrival near large in-stream features is visible in WS01 during all injections. In WS03, well H5 (near the stream centerline in the upstream half of the study reach) always exhibits longer mean arrival times than other monitoring locations. We attribute this anomalous behavior to the well-being located at the upwelling end of a flow path hypothesized to go below a large boulder visible at this location. Notation of m* indicates a slope that is significant (i.e., 0 is not within the 95% confidence interval for linear regression slope).

3.2. Hyporheic Transfer Functions: Mean Arrival Times

Ranges of observed mean arrival times (M_1) along hyporheic flow paths are larger in WS01 compared to WS03 (Figure 5). In both watersheds, the consistent peak increases in SC (wells E4, E5, W6, G5 in WS01; H4 in WS03) are also visible for M_1. These wells are anomalous relative to the surrounding wells, with rapid arrivals at the wells identified at wells E4, E5, W6, and G5 in WS01 and slow arrival at well G5 in WS03. Mean arrival time generally increases with distance from the stream centerline in WS01 for all injections and decreases with distance from the stream in WS03 for all injections. Slopes between distance from the stream and mean arrival time are significant for all injections in WS01 and none in WS03. The study watersheds are significantly different for injections 2 and 4 ($p_{ANOVA} < 0.001$ for both injections, $p_{KW} = 0.0012$ and <0.001 for injections 2 and 4, respectively), but not for injections 1 and 3 ($p_{ANOVA} = 0.12$ and 0.16, $p_{KW} = 0.089$ and 0.056, for injections 1 and 3, respectively; Figure 5). Overall for mean arrival time, there are significant differences between injections for WS01 ($p_{ANOVA} < 0.001$; $p_{KW} < 0.001$ for M_1; Figure 4c) but not for WS03 ($p_{ANOVA} = 0.96$; $p_{KW} = 0.92$ for M_1; Figure 4d).

3.3. Hyporheic Transfer Functions: Temporal Variance

Temporal variance (μ_2) of the transfer functions (transport along hyporheic flow paths) is generally larger in WS01 compared to WS03 (Figure 6). There are significant differences in μ_2 between the watersheds for injections 1, 2, and 4 ($p_{ANOVA} = 0.011$, 0.049 and <0.001, $p_{KW} = 0.0024$, 0.039 and <0.001 for injections 1, 2, and 4, respectively), but not for injection 3 ($p_{ANOVA} = 0.071$, $p_{KW} = 0.40$). For all stream discharges, temporal

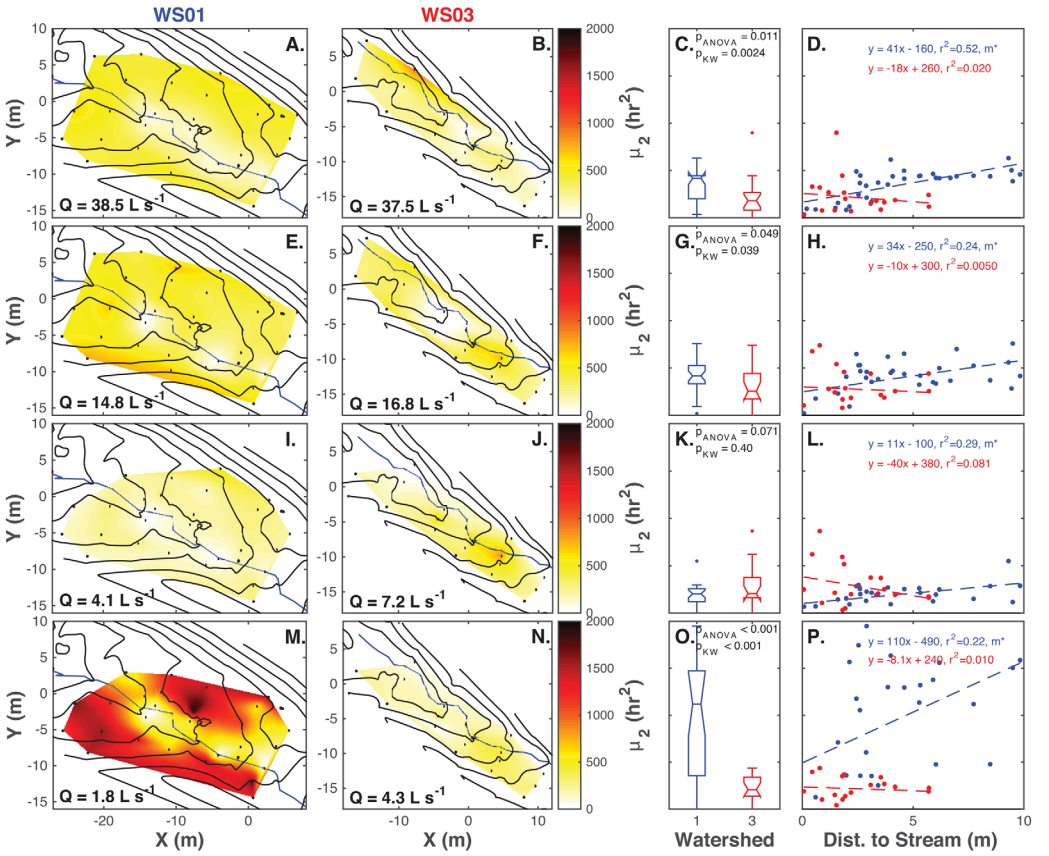

Figure 6. Temporal variance for each well. In WS01, significant positive relationships between distance from stream centerline and temporal variance were found. In WS03, these relationships were always negative, though the slopes were not significant. Significant differences between WS01 and WS03 exist for temporal variance only for injection 4. In WS01 during injection 4, the lowest discharge condition observed, the flow paths in the riparian zone had much larger temporal variance that observed during previous injections, possibly owing to diurnal fluctuations in hydraulic gradients causing increased spreading during this injection. Notation of m* indicates a slope that is significant (i.e., 0 is not within the 95% confidence interval for linear regression slope).

variance increases with increasing distance from the stream centerline for WS01 (statistically significant positive slope between distance and temporal variance) and decreases with increasing distance for WS03 (negative but not significant slope between distance and temporal variance for all discharges). Overall for temporal variance, there are significant differences between injections for WS01 ($p_{ANOVA} < 0.001$; $p_{KW} < 0.001$ for μ_2; Figure 4e) but not for WS03 ($p_{ANOVA} = 0.60$; $p_{KW} = 0.49$ for μ_2; Figure 4f).

3.4. Relationship Between Hyporheic Transfer Function Metrics and Stream Discharge

For both WS01 and WS03, the M_1 of the hyporheic flow paths estimated at each well generally decrease with increasing discharge (28 of 33 wells in WS01, 14 of 19 wells in WS03; Figure 7). There are significant differences between best-fit slopes for M_1 with discharge for the two watersheds ($p_{ANOVA} = 0.0031$; $p_{KW} = 0.0012$), with WS01 being generally more sensitive to changes in discharge (larger variability in slopes). Although there is an overall negative relationship between stream discharge and hyporheic M_1 values in both catchments, slopes not statistically significant. For μ_2, data from both catchments show generally negative relationships with discharge (23 of 33 and 15 of 19 for WS01 and WS03, respectively), but again, no slopes are statistically significant. The difference in slopes for μ_2 with discharge between watersheds is significant based on an ANOVA test ($p_{ANOVA} = 0.034$), but not a Kruskal-Wallis test ($p_{KW} = 0.089$); WS01 generally exhibits larger magnitude slopes with discharge than WS03. In both cases, locations with a zero-slope indicate transfer functions that are not significantly related to hydrologic changes through seasonal base flow recession (Figure 8).

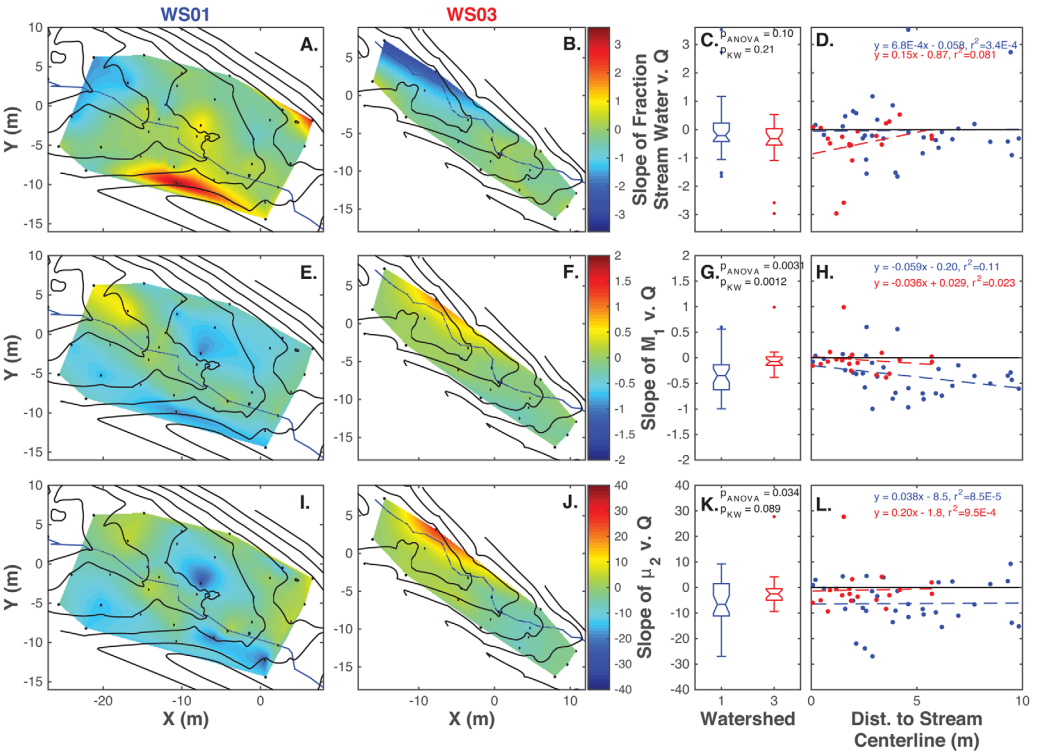

Figure 7. Relationships between temporal metrics and discharge. Increasing discharge is generally associated with decreasing mean arrival time and decreasing temporal variance in both WS01 and WS03. WS01 exhibited overall more sensitivity to discharge than WS03 (based on mean slope of relationships with discharge) for both mean arrival time and temporal variance, and wider ranges in the relationship. Differences between WS01 and WS03 were significant for mean arrival time using both ANOVA and Kruskal-Wallis tests, and for temporal variance using the Kruskal-Wallis test. No trends with distance from the stream centerline were significant for either watershed or metric, though general trends of decreasing slopes between discharge and mean arrival time and increasing slopes between temporal variance and discharge were observed with increasing distance from the channel. Notation of m* indicates a slope that is significant (i.e., 0 is not within the 95% confidence interval for linear regression slope).

4. Discussion

4.1. Interactions of Discharge With Geologic Setting may Result in Dynamic Transport Processes

The observed spatial and temporal patterns in hyporheic transport reflect the interaction of hydrologic forcing with the geologic setting in each catchment. Declining stream discharge in the catchment can be attributed to a combination of increasing evapotranspiration demand in the riparian zone and hillslopes and decreasing drainage from hillslope soils through the season [*Bond et al.*, 2002; *Wondzell et al.*, 2007, 2010]. This pattern is marginally apparent in our study wells where riparian water levels were reasonably constant through the season. Despite the order of magnitude decrease in discharge through the study period and the associated declines in valley bottom water tables, valley bottom hydraulic gradients remained generally consistent through the season [*Wondzell*, 2006; *Voltz et al.*, 2013]. Given that the geologic setting (e.g., streambed morphology, valley bottom hydrogeologic properties) remained static through the study period, we propose five mechanisms to explain the changes (or lack of change) in transport metrics observed through base flow recession (Figure 8). Each mechanism is detailed below as a perceptual model, presented with the goal of formulating process-based explanations for observed field dynamics [*McGlynn et al.*, 2002] based on our subjective understanding of the system [*Sivapalan*, 2003; *Wagener et al.*, 2007]. As such, these models represent field-based hypotheses that are a necessary step in explaining the mechanistic function of hydrological systems [*Burt and McDonnell*, 2015].

First, although the observed cross-valley and down-valley gradients remained nearly constant, riparian water levels were observed to decrease through the season [*Voltz et al.*, 2013]. The change in water level results in a change in the effective subsurface hydraulic conductivity (K; Figure 8a). The water table fell below several of our wells through the season, suggesting changes in the K field with groundwater table elevation may be occurring. Dynamic connectivity of hillslopes and streams has been observed in other

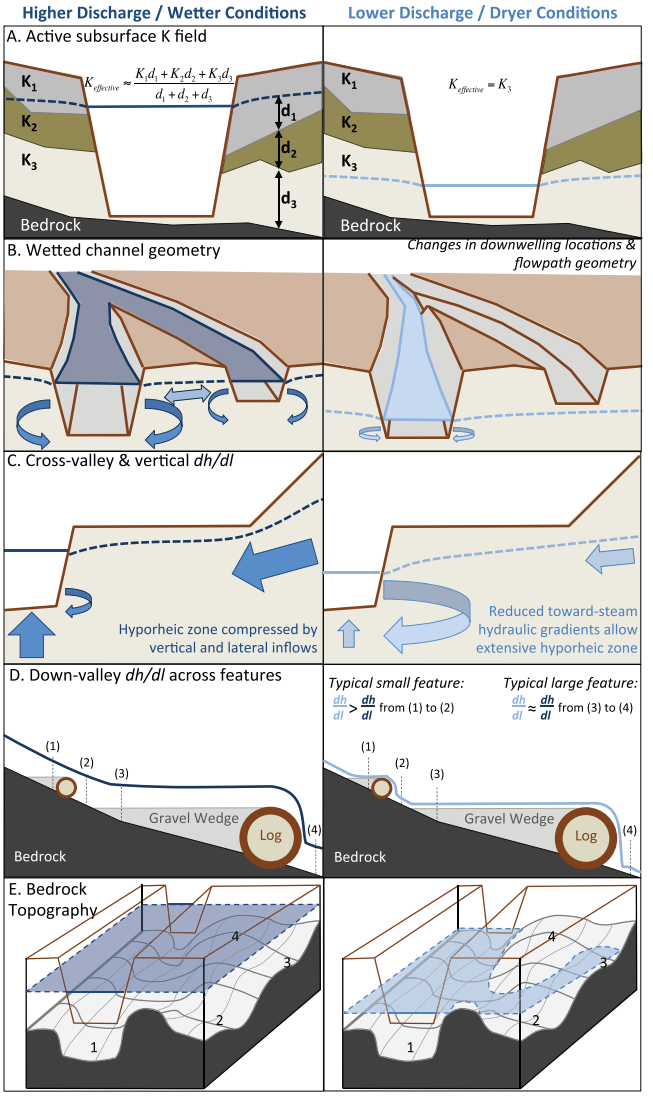

Figure 8. Conceptual models of five interactions between valley bottom hydrology and geologic setting that may explain the results observed in this study. (a) Changes in riparian water level may activate different portions of the subsurface, amplifying the impact of near-surface heterogeneity. (b) Changes in wetted geometry with discharge, such as activation of side channels, may change up and downwelling locations of hyporheic flow paths, and interactions though in-stream bars. (c) Changes in ambient groundwater discharge and lateral hydraulic gradients have been shown to compress hyporheic flow paths in some systems. (d) Changes in the effective roughness of a channel with discharge may alter exchange dynamics near small features, but large features such as fallen logs or boulders may generate hydraulic gradients that are insensitive to in-stream discharge. (e) Bedrock topography may cause increasingly complex flow paths, particularly under low flow conditions where local bedrock highs may provide a physical barrier between locations.

mountain catchments [e.g., *Jencso et al.*, 2009] with varying impacts on riparian transport [*Jencso et al.*, 2010; *Pacific et al.*, 2010]. As the water table falls in the riparian zone, transport may be through a different portion of the heterogeneous K field. We find this mechanism unlikely to explain the patterns observed in this study. In the study catchments, the water table height fell only 10–15 cm across the range of studied stream discharges. While it is possible, it is hard to envision that this relatively small change in water table height would lead to flow being restricted to layers of lower hydraulic conductivity sediment. Furthermore, the bulk of the sediment filling the floor of this steep narrow valley was likely emplaced by debris flows when large logs wedged across the valley floor, formed logjams, and captured large wedges of sediment [e.g., *Swanson and Jones*, 2002]. As such, we would expect most of the valley floor sediment to be well mixed and not deposited in distinct layers typical of fluvial floodplains in lower-gradient systems.

Second, with changes in discharge, the wetted geometry of the stream itself, and possibly the origin of downwelling hyporheic flow paths, changed (Figure 8b). Although changes in stage over the study period were small, the combination of slightly lowered water tables and stream discharge were sufficient to cause a side channel near the head of the study reach in WS01 to go dry. This would mark a substantial and abrupt state change in the location and head gradients where hyporheic flow paths originated near the head of our study reach. This change in downwelling location would be expected to yield changes in hyporheic residence times in the down-valley subsurface. Because we are unable to directly observe which wells are directly linked to which downwelling zones, we cannot predict exactly how these changes in channel configuration should impact the hyporheic zone; although we hypothesize such changes could be large. Furthermore, the largest changes in hyporheic transport metrics in our study were observed between tracer tests conducted at the second-lowest and the lowest stream discharges studied and only in WS01, the only study reach that had multiple channels. However, if changes in channel configuration controlled the observed changes in hyporheic transport metrics across the valley bottom, we would have expected to observe differences in M_1 in both near-stream and more distant wells. Instead, we found observation

locations nearest the stream channel have the smallest sensitivity of M_1 to discharge (determined as the smallest magnitudes in slopes of metrics with discharge; Figure 7), with increasing sensitivity to discharge with increasing distance from the channel. We interpret, then, that the wells nearest the stream are dominated by the static hydraulic gradients and exchange is driven by large roughness features in the valley bottom. This can be seen by the time-invariant behavior at wells E4, E5, W6, and G5 in WS01 and H4 in WS03. In WS01, these locations are dominated by their location near steps and riffles, which maintain large hydraulic gradients through the season. In WS03, well H4 appears to be located at the end of a long flow path that we believe to be under or around a large, visible boulder that creates a step of more than 1 m elevation change in the stream channel. In both cases, we attribute strong, time-invariant hydraulic gradients arising due to the streambed morphology dominance as opposed to dynamic hydrologic forcing.

Third, cross-valley and vertical hydraulic gradients oriented toward the stream can compress both vertical and lateral hyporheic exchange, countering the gradients away from the stream at downwelling locations (Figure 8c). Several conceptual models [*Hynes*, 1983; *Meyer et al*., 1988; *Vervier et al*., 1992; *Hakenkamp et al*., 1993; *Palmer*, 1993; *White et al*., 1993] and simulations [*Cardenas and Wilson*, 2006, 2007; *Boano et al*., 2008; *Kalbus et al*., 2008; *Trauth et al*., 2013] demonstrate how this hyporheic compression should occur. Still, our findings agree with those of several others, failing to confirm compression of hyporheic flow paths under periods of higher discharge [*Harvey and Bencala*, 1993; *Storey et al*., 2003; *Wondzell*, 2006; *Ward et al*., 2012]. In our study, the highest sensitivity to discharge was primarily observed at the riparian-hillslope transition, suggesting those flow paths may vary with hydrologic forcing despite the time-invariant transport metrics observed near the stream channel. *Jencso et al*. [2009] showed that hydrologic connectivity of hillslopes and valley bottoms was neither spatially nor temporally constant. Rather, lateral inputs from hillslopes adjacent to the stream were controlled by catchment wetness and the size of the accumulated hillslope area draining to any point along the stream channel. At very high catchment wetnesses, even small upslope accumulated areas maintained hydrologic connectivity and presumably supplied lateral inputs to the valley bottom. Under dry conditions, most of the valley bottom was disconnected from the adjacent hillslopes in their study. If changes in lateral inputs were a major factor controlling tracer movement through the valley bottom of WS01, we would expect the influence of changing wetness to occur differentially, depending on the upslope accumulated area supplying water to any location within our well network, and that changes should occur as a gradient between high, intermediate, and low stream discharges. We did not observe this. Rather, there was no discernible change in the overall shape of the water table along the hillslope-riparian boundary over the range of stream discharges we studied. As a result, hyporheic flow path M_1 was relatively time-invariant as discharge decreased from 38 to 4.1 L/s, only changing as discharge decreased further to 1.8 L/s in our last injection (Figure 4c). Thus the observed changes are inconsistent with those expected where lateral inputs are the primary control on tracer arrival times near the hillslope-riparian boundary.

Fourth, the size of individual roughness elements may control variability in response to changing discharge (Figure 8d). Hyporheic exchange has been empirically related to Darcy-Weisbach friction factor and stream power [*Zarnetske et al*., 2007] as well as water surface concavity [*Anderson et al*., 2005], suggesting variability in the stream water surface profile is an important predictor of hyporheic exchange. For small roughness elements, large discharges may overwhelm the feature itself [e.g., *Church and Zimmermann*, 2007]. The result of the more linear water surface profile is reduced down-valley hydraulic gradients across the feature, yielding reduced hyporheic exchange flux. For large roughness elements, the hydraulic gradient across the feature is maintained at an approximately constant level under a range of flow conditions. In WS01 and WS03, the large-scale roughness elements are commonly downed trees or logs and large boulders or bedrock outcrops. Based on visual inspection, the locations of large roughness elements are correlated with time-invariant metrics in the subsurface, supporting this as a possible mechanism. This is reflected by the insensitivity of hyporheic transport to stream discharge that is ubiquitous in WS03 and near the stream in WS01. Only flow paths that are near the valley-hillslope transition (i.e., far from the persistent gradients imparted by the large in-stream roughness elements) were time-variable with discharge. *Storey et al*. [2003] showed that, at high flows, pool-riffle sequences can be drowned out and, when combined with substantial increases of lateral groundwater inputs, dramatically limit hyporheic exchange. In our study, despite large changes in discharge, variation in stream stage was, at most, 17.2 cm in WS01 and 18.3 cm in WS03. These changes were insufficient to drown out roughness elements such as large logs and boulders that formed

steps in the channels of our study reaches based on visual inspection during the field studies. If this were the primary explanation for the observed behavior, we would have expected to see the largest changes between high and intermediate stream discharges in both watersheds. Instead, we saw the largest changes in M_1 only in WS01 and only between the tracer tests at the two lowest discharges (4.1 and 1.8 L/s) not sufficient to drown out large roughness elements.

Fifth, we hypothesize that interactions between water table height and the topography of the underlying bedrock could have a substantial influence on the flow network through the hyporheic zone (Figure 8e), similar to the mechanisms shown on hillslopes underlain by bedrock with complex topography [e.g., *McDonnell et al*., 1996; *Freer et al*., 2002; *Graham et al*., 2010]. A section upstream of our study reach in WS03 was scoured to bedrock following a debris flow in 1996, revealing a complex bedrock surface below riparian alluvial material (see "bedrock reach" described in *Johnson* [2004]; *Gooseff et al*. [2005]; *Argerich et al*. [2011]). In some places, the exposed bedrock confines the stream into narrow, incised channels on the order of 20 cm in width during low discharges. In other places, the bedrock forms broad smooth shelves across the width of the valley resulting in sheet flow. Additionally, the valley-edge bedrock topography does not slope smoothly downstream, but is characterized by short rises and hollows. Presumably, the bedrock that underlays both study reaches in WS01 and WS03 has similarly complex topography. If the water table is high enough to be spatially continuous above the bedrock surface, then we would expect more spatially uniform down-valley transport in the subsurface. While in some places the water table lies only a few cm above the bedrock, our observations show that water table elevation changes of as little as 10–15 cm are sufficient enough to completely dry out some monitoring locations. This drying does not occur uniformly through the network, suggesting that this may occur only in locations of bedrock topographic highs (as small mound, ridge or dike, such as point 4 in Figure 8e) but not lows (as in shallow pools or channels such as points 1 and 2 in Figure 8e). Under this bedrock topography situation, small changes in water table elevations could have large impacts on the hyporheic and riparian flow net. For example, we would expect such changes to occur preferentially at locations more distant from the stream—places where hyporheic exchange is not as directly coupled to stream hydrodynamics. Thus we would expect these changes to occur along the valley margins in WS01 but not in the much narrower WS03. As valley bottom water table falls and interacts with bedrock topography, bedrock ridges could block down-valley flow and/or serve to channelize flow toward bedrock lows (such as point 3 in Figure 8e). Our observations of the largest changes in transport metrics occurring in WS01 between the second-lowest and lowest discharge conditions support this mechanism, in which distal wells both went dry and showed the largest changes in M_1 with decreasing discharge.

4.2. Possible Limitations of Interpreting Direct Observations in the Well Network

We note three additional, related possibilities that are limitations of direct observation of solute tracer concentrations in the well network. First, each well is subject to its own window of detection limitation [sensu *Harvey et al*., 1996; *Harvey and Wagner*, 2000]. The observed time series at the well is a function of the concentration and duration of injection, sensitivity of instrumentation, and the actual transport processes occurring along the flow paths (e.g., dilution by unlabeled water). In our study, as in those focused on stream solute tracers, the repeated methodology of injections does not necessarily guarantee directly comparable results. In WS03, a distributed study using electrical geophysics suggests that overall flow field geometry was generally unchanged, extending across the same spatial domain across all four injections [*Ward et al*., 2014]. In both WS01 and WS03, the hydraulic gradients were reasonably constant through the season [*Voltz et al*., 2013], though less information is available regarding flow path-scale dynamics in that catchments. Still, we expect that our subsurface observations were, to some degree, subject to window of detection limitations.

Second, the use of fixed observation locations within a dynamic flow field may obscure hyporheic and riparian behavior. For example, flow path geometry could change such that a well initially located near the head of a hyporheic flow path is later at a point near the tail of a flow path (or vice versa). This mechanism would change timescales of observation because of a changing geometry of flow paths, not necessarily a change in processes occurring along a fixed flow path. In our study, hydraulic gradients in the valley bottom were largely constant through the season [*Voltz et al*., 2013], from which we interpret this mechanism is not expected to be dominant in our study. Still, we note that it is important to consider time-variable possibilities in interpretation of results in other systems.

Third, we assumed the downwelling solute tracer time series was well-approximated by the in-stream solute tracer time series adjacent to each well transect. Thus, our calculations strictly yield descriptors of the difference in temporal moments that is caused by transport along a hyporheic flow path that would not have otherwise resulted from transport in the stream. The implicit assumption is that transformation of the time series along the stream between the downwelling location and transect is minimal, thereby assigning all change to transport along the hyporheic flow path. For wells and pizeometers in and near the stream channel, this assumption is appropriate because the downwelling flow path is likely to originate near the stream, where negligible in-stream modification of the downwelling signal occurs over these short distances. For wells located at large distances from the stream, this assumption is valid because the advective timescale of transport in the hyporheic zone is much slower than in-stream transport, reducing the impact of small differences in downwelling time series on longer flow paths. Future work to reduce uncertainty associated with this assumption would explicitly address subsurface flow path geometry and the distribution of downwelling locations along the stream channel.

4.3. Down-Valley Transport is Independent of Stream Discharge in Headwater Mountain Streams

Despite order of magnitude changes in discharge, we found relatively little variation in transport along hyporheic flow paths (Figures 5–7). Indeed, subsurface transport was largely insensitive to in-stream discharge (low magnitude slopes in Figure 7). These patterns are explained by a conceptual model in which both the stream and subsurface flow in parallel along the valley bottom. The subsurface flow remains nearly constant through the season given the largely unchanging geologic setting at the valley scale (e.g., hydraulic conductivity field, large roughness elements, fixed bedrock constraint) and down-valley hydraulic gradients. In contrast, the surface stream flow represents the down-valley discharge that is beyond the capacity of the subsurface, transporting excess flow down the valley. As such, stream discharge can be highly dynamic without the requirement of corresponding dynamics in subsurface transport timescales. Reductions in discharge from the hillslope to the stream through base flow recession explain decreasing water levels in the valley bottom, and overall decreases in catchment discharges. In WS03, the highly constrained valley is dominated by geological control; lateral inflows have relatively little impact on valley bottom transport at any location. In WS01, the near-stream transport is functionally isolated from the hillslope, with constant down-valley and hyporheic exchange processes through the four experiments. Near the valley walls, changing lateral inflows from the hillslopes interact with valley bottom bedrock topography, particularly during the lowest flows. In these locations, the steeper relationships with discharge may actually indicate dominance by hillslope inputs or by underlying bedrock topography. Stream discharge measures catchment-integrated response, but its recession through the season is explained by similar reductions in flux from hillslopes to the valley bottom. The negative relationships with discharge at the valley walls likely indicate negative relationships with hillslope discharge to the valley bottom, not stream discharge itself. Therefore, conceptual models must reflect the interactions between dynamic hydrologic forcing and geologic setting to improve solute transport predictions spanning systems and several spatial scales.

While most of the valley bottom responses we observed were time-invariant—strongly controlled by channel morphology interacting with the hyporheic flow net in ways that did not change with changing stream discharge—some metrics describing hyporheic exchange did change through time. Even so, we do not see evidence that these are directly controlled by hydrodynamics (in the classical sense of interactions of fluid forces with solid bodies and the motion of fluids). Such mechanisms have been observed for other types of morphologies, including bed forms considered in pumping-exchange models [*Elliott and Brooks*, 1997a,b]. Whereas hydrodynamics implies that changes in discharge and/or in-stream velocity lead to changes in hyporheic exchange, we define here a different suite of process dynamics. In our system, and in the preceeding paragraphs, we detail how changes in valley bottom hydrology appear to change the way the surface and subsurface flow field interacts with the morphologic setting. We refer to these changes as "hydrogeomorphic responses" so as to conceptually distinguish them from "hydrodynamic responses" that have been well described in the literature. This is consistent with the definition of hydrogeomorphology as "an interdisciplinary science that focuses on the interaction and linkage of hydrologic processes with landforms or earth materials and the interaction of geomorphic processes with surface and subsurface water in temporal and spatial dimensions" [*Sidle and Onda*, 2004, pg. 597], emphasizing interactions between hydrologic and geomorphic controls on observed process dynamics.

5. Conclusions

In this study, we set out to address two key questions. First, we asked how hyporheic transit times in a valley bottom change through seasonal base flow recession? We found hyporheic flow paths in WS01 change in response to discharge more than those in WS03, with increased sensitivity as distance from the stream channel increased. Near the channel in WS01 we found transport along hyporheic flow paths was insensitive to discharge, with little change in transport metrics despite large changes in discharge and riparian water level. In WS03, we found almost ubiquitous time-invariance in transport metrics. Second, we asked how does the time-variability in hyporheic transit time distributions differ as a function of valley constraint within and between catchments? We found valley constraint in WS03 resulted in time-invariant transport, while the wider alluvial valley in WS01 did have time-variable behavior. For WS03 and the near-stream area in WS01, geologic controls dominate hyporheic behavior, with little to no impact of hydrologic variability. In contrast, flow paths far from the stream in the wider WS01 were sensitive to discharge, likely an integration of hillslope discharges to the riparian zone with valley bottom hydrology driven by the stream and upstream inputs.

We expected that monitoring well observations would suggest temporally variable transit time distributions between the injection location and monitoring location. This was observed, and is attributed primarily to the channel stream transport dynamics occurring between the injection location at the observation location. We further expected that static morphology and valley bottom hydraulic gradients would manifest as constant hyporheic transport processes. This was confirmed for flow paths in the highly constrained WS03, and near large roughness elements in WS01. For the riparian-hillslope transition in the broader WS01, systematic changes with discharge were observed, and attributed to changing discharge from the hillslopes to the valley bottom. In-stream processes do not appear to be linked to the observations at these distal wells given the zone of time-invariant transport adjacent to the stream. We attribute the observed sensitivity to discharge as an indication of sensitivity to hillslope contributions to the valley bottom, which are expected to be correlated in time with in-stream discharge.

Overall, this study demonstrates: (1) near-stream hyporheic flow path transport is time-invariant across the discharge conditions studied because hydraulic gradients are constant across large in-stream morphologic features; (2) riparian zone hyporheic transport is time-invariant in highly constrained valley bottoms, and time-variable near the hillslope interface in wider valley bottoms; and (3) isolation of hyporheic and in-stream solute transport processes is important for study of hyporheic hydrodynamics. As such, refinement of conceptual models to include interactions between hydrologic forcing and geologic setting is a requisite step toward making meaningful predictions of hyporheic and riparian processes in mountain stream networks.

Acknowledgments

Data and facilities were provided by the H.J. Andrews Experimental Forest research program, funded by the National Science Foundation's (NSF's) Long-Term Ecological Research Program (DEB 1440409), U.S. Forest Service Pacific Northwest Research Station, and Oregon State University. Gooseff, Singha, and Ward were supported by the NSF's Hydrologic Sciences program, under grant EAR 0911435. *Wondzell* was supported by NSF grant EAR 1417603. Tools for solute tracer time series analyses were developed by Ward and others with support provided in part by the National Science Foundation (NSF) grant EAR 1331906 for the Critical Zone Observatory for Intensively Managed Landscapes (IML-CZO), a multiinstitutional collaborative effort. Any opinions, findings, and conclusions or recommendations expressed in this material are those of the authors and do not necessarily reflect the views of the National Science Foundation, U.S. Forest Service, or the H.J. Andrews Experimental Forest. Precipitation and discharge data are available from the H.J. Andrews Experimental Forest Data Catalog (http://andrewsforest.oregonstate.edu/). Topographic survey, in-stream specific conductance, and down-well specific conductance data are available upon request to the corresponding author. The authors declare no conflicts of interest.

References

Anderson, J. K., S. M. Wondzell, M. N. Gooseff, and R. Haggerty (2005), Patterns in stream longitudinal profiles and implications for hyporheic exchange flow at the H. J. Andrews Experimental Forest, Oregon, USA, *Hydrol. Processes*, *19*(15), 2931–2949.

Argerich, A., et al. (2011), Quantification of metabolically active transient storage (MATS) in two reaches with contrasting transient storage and ecosystem respiration, *J. Geophys. Res.*, *116*, G03034, doi:10.1029/2010JG001379.

Boano, F., R. Revelli, and L. Ridolfi (2008), Reduction of the hyporheic zone volume due to the stream-aquifer interaction, *Geophys. Res. Lett.*, *35*, L09401, doi:10.1029/2008GL033554.

Bond, B. J., J. a. Jones, G. Moore, N. Phillips, D. Post, and J. J. McDonnell (2002), The zone of vegetation influence on baseflow revealed by diel patterns of streamflow and vegetation water use in a headwater basin, *Hydrol. Processes*, *16*(8), 1671–1677, doi:10.1002/hyp.5022.

Burt, T. P., and J. J. McDonnell (2015), Whither field hydrology? The need for discovery science and outrageous hydrological hypotheses, *Water Resour. Res.*, *51*, 5919–5928, doi:10.1002/2014WR016839.

Cardenas, M. B., and J. L. Wilson (2006), The influence of ambient groundwater discharge on exchange zones induced by current-bedform interactions, *J. Hydrol.*, *331*(1-2), 103–109, doi:10.1016/j.jhydrol.2006.05.012.

Cardenas, M. B., and J. L. Wilson (2007), Exchange across a sediment-water interface with ambient groundwater discharge, *J. Hydrol.*, *346*(3-4), 69–80.

Choi, J., J. W. Harvey, and M. H. Conklin (2000), Characterizing multiple timescales of stream and storage zone interaction that affect solute fate and transport in streams, *Water Resour. Res.*, *36*(6), 1511–1518.

Church, M., and A. Zimmermann (2007), Form and stability of step-pool channels: Research progress, *Water Resour. Res.*, *43*, W03415, doi:10.1029/2006WR005037.

Covino, T. P., B. L. McGlynn, and J. Mallard (2011), Stream-groundwater exchange and hydrologic turnover at the network scale, *Water Resour. Res.*, *47*, W12521, doi:10.1029/2011WR010942.

D'Angelo, D. J., J. R. Webster, S. V Gregory, J. L. Meyer, A. D. J. D. Angelo, J. R. Webster, S. V Gregory, and J. L. Meyer (1993), Transient storage in appalachian and cascade mountain streams as related to hydraulic characteristics, *J. N. Am. Benthol. Soc.*, *12*(3), 223–235, doi:10.2307/1467457.

Drummond, J. D., T. P. Covino, a. F. Aubeneau, D. Leong, S. Patil, R. Schumer, and a. I. Packman (2012), Effects of solute breakthrough curve tail truncation on residence time estimates: A synthesis of solute tracer injection studies, *J. Geophys. Res.*, *117*, G00N08, doi:10.1029/2012JG002019.

Dyrness, C. T. (1969), Hydrologic properties of soils on three small watersheds in the western Cascades of Oregon, *USDA For. Serv. Res. Note PNW-111*, 17 pp.
Elliott, A. H., and N. H. Brooks (1997a), Transfer of nonsorbing solutes to a streambed with bed forms: Laboratory experiments, *Water Resour. Res.*, *33*(1), 123–136.
Elliott, H., and N. H. Brooks (1997b), Transfer of nonsorbing solutes to a streambed with bed forms: Theory, *Water Resour. Res.*, *33*(1), 123–136.
Findlay, S. (1995), Importance of surface-subsurface exchange in stream ecosystems: The hyporheic zone, *Limnol. Oceanogr.*, *40*(1), 159–164.
Fischer, H. B. (1979), *Mixing in Inland and Coastal Waters*, Academic Press, San Diego, Calif.
Freer, J. E., K. J. Beven, J. J. McDonnell, and N. E. Peters (2002), The role of bedrock topography on subsurface stormflow., *Water Resour. Res.*, *38*(12), 1269, doi:10.1029/2001WR000872.
Gooseff, M. N., D. M. McKnight, R. L. Runkel, J. H. Duff, and D. Valleys (2004), Denitrification and hydrologic transient storage in a glacial meltwater stream, McMurdo Dry Valleys, *Antarctica, Limnol. Oceanogr.*, *49*(5), 1884–1895.
Gooseff, M. N., J. LaNier, R. Haggerty, and K. Kokkeler (2005), Determining in-channel (dead zone) transient storage by comparing solute transport in a bedrock channel–alluvial channel sequence, Oregon, *Water Resour. Res.*, *41*, W06014, doi:10.1029/2004WR003513.
Gooseff, M. N., J. K. Anderson, S. M. Wondzell, J. LaNier, and R. Haggerty (2006), A modelling study of hyporheic exchange pattern and the sequence, size, and spacing of stream bedforms in mountain stream networks, Oregon, USA, *Hydrol. Processes*, *20*(11), 2443–2457.
Graham, C. B., R. a. Woods, and J. J. McDonnell (2010), Hillslope threshold response to rainfall: (1) A field based forensic approach, *J. Hydrol.*, *393*(1-2), 65–76, doi:10.1016/j.jhydrol.2009.12.015.
Hakenkamp, C. C., H. M. Valett, and A. J. Boulton (1993), Perspectives on the hyporheic zone: Integrating hydrology and biology. Concluding remarks, *J. N. Am. Benthol. Soc.*, *12*(1), 94–99, doi:10.2307/1467683.
Harman, C. J. (2015), Time-variable transit time distributions and transport: Theory and application to storage-dependent transport of chloride in awatershed, *Water Resour. Res.*, *51*, 1–30, doi:10.1002/2014WR015707.
Harvey, J. W., and K. E. Bencala (1993), The effect of streambed topography on surface-subsurface water exchange in mountain catchments, *Water Resour. Res.*, *29*(1), 89–98.
Harvey, J. W., and B. J. Wagner (2000), Quantifying hydrologic interactions between streams and their subsurface hyporheic zones, in *Streams and Ground Waters*, edited by J. B. Jones and P. J. Mulholland, pp. 3–44, Academic Press, San Diego, Calif.
Harvey, J. W., B. J. Wagner, and K. E. Bencala (1996), Evaluating the reliability of the stream tracer approach to characterize stream-subsurface water exchange, *Water Resour. Res.*, *32*(8), 2441–2451.
Hynes, H. B. N. (1983), Groundwater and stream ecology, *Hydrobiologia*, *100*(1), 93–99.
Jackson, T. R., R. Haggerty, and S. V. Apte (2013), A fluid-mechanics based classification scheme for surface transient storage in riverine environments: Quantitatively separating surface from hyporheic transient storage, *Hydrol. Earth Syst. Sci.*, *17*(7), 2747–2779, doi:10.5194/hess-17-2747-2013.
Jencso, K. G., B. L. McGlynn, M. N. Gooseff, S. M. Wondzell, K. E. Bencala, and L. A. Marshall (2009), Hydrologic connectivity between landscapes and streams: Transferring reach-and plot-scale understanding to the catchment scale, *Water Resour. Res.*, *45*, W04428, doi:10.1029/2008WR007225.
Jencso, K. G., B. L. McGlynn, M. N. Gooseff, K. E. Bencala, and S. M. Wondzell (2010), Hillslope hydrologic connectivity controls riparian groundwater turnover: Implications of catchment structure for riparian buffering and stream water sources, *Water Resour. Res.*, *46*, W10524, doi:10.1029/2009WR008818.
Johnson, S. L. (2004), Factors influencing stream temperatures in small streams: Substrate effects and a shading experiment, *Can. J. Fish. Aquat. Sci.*, *61*(6), 913–923.
Kalbus, E., C. Schmidt, J. W. Molson, F. Reinstorf, and M. Schirmer (2008), Influence of aquifer and streambed heterogeneity on the distribution of groundwater discharge, *Hydrol. Earth Syst. Sci. Discuss.*, *5*(4), 2199–2219, doi:10.5194/hessd-5-2199-2008.
Kasahara, T., and S. M. Wondzell (2003), Geomorphic controls on hyporheic exchange flow in mountain streams, *Water Resour. Res.*, *39*(1), 1005, doi:10.1029/2002WR001386.
Käser, D. H., A. M. Binley, A. L. Heathwaite, and S. Krause (2009), Spatio-temporal variations of hyporheic flow in a riffle-step-pool sequence, *Hydrol. Processes*, *23*(15), 2138–2149.
Lewandowski, J., G. Lischeid, and G. Nutzmann (2009), Drivers of water level fluctuations and hydrological exchange between groundwater and surface water at the lowland River Spree (Germany): Field study and statistical analyses, *Hydrol. Processes*, *23*, 2117–2128, doi:10.1002/hyp.7277.
Maloszewski, P., and A. Zuber (1982), Determining the turnover time of groudwater systems with the aid of environmental tracers: 1. Models and their applicability, *J. Hydrol.*, *57*, 207–231.
Mason, S. J. K., B. L. McGlynn, and G. C. Poole (2012), Hydrologic response to channel reconfiguration on Silver Bow Creek, Montana, *J. Hydrol.*, *438-439*, 125–136.
McDonnell, J. J., J. Freer, R. Hooper, C. Kendall, D. Burns, K. J. Beven, and J. Peters (1996), New method developed for studying flow on hillslopes., *Eos Trans. AGU*, *77*(47), 465–472, doi:10.1029/96EO00306.
McGlynn, B. L., J. J. McDonnell, and D. D. Brammer (2002), A review of the evolving perceptual model of hillslope flowpaths at the Maimai catchments, New Zealand, *J. Hydrol.*, *257*, 1–26.
McGuire, K. J., and J. J. McDonnell (2006), A review and evaluation of catchment transit time modeling, *J. Hydrol.*, *330*(3-4), 543–563, doi:10.1016/j.jhydrol.2006.04.020.
Meyer, J. L., W. H. McDowell, T. L. Bott, J. W. Elwood, C. Ishizaki, J. M. Melack, B. L. Peckarsky, B. J. Peterson, and P. A. Rublee (1988), Elemental dynamics in streams, *J. N. Am. Benthol. Soc.*, *7*(4), 410–432.
Pacific, V. J., K. G. Jencso, and B. L. McGlynn (2010), Variable flushing mechanisms and landscape structure control stream DOC export during snowmelt in a set of nested catchments, *Biogeochemistry*, *99*(1), 193–211, doi:10.1007/s10533-009-9401-1.
Packman, A. I., and K. E. Bencala (2000), Modeling surface-subsurface hydrological interactions, in *Streams and Ground Waters*, edited by J. B. Jones and P. J. Mulholland, pp. 45–80, Academic Press, San Diego, Calif.
Packman, A. I., and M. Salehin (2003), Relative roles of stream flow and sedimentary conditions in controlling hyporheic exchange, *Hydrobiologia*, *494*(1), 291–297.
Packman, I. I., A. I. Packman, and N. H. Brooks (2001), Hyporheic exchange of solutes and colloids with moving bed forms, *Water Resour. Res.*, *37*(10), 2591–2605.
Palmer, M. A. (1993), Experimentation in the Hyporheic Zone: Challenges and Prospectus, *J. N. Am. Benthol. Soc.*, *12*(1), 84–93.
Payn, R. A. (2009), *Stream Hydrologic Characterizations Across Time and Space*, Colo. Sch. of Mines, Golden.
Ryan, R. J., A. I. Packman, and C. Welty (2004), Estimation of solute transport and storage parameters in a stream with anthropogenically produced unsteady flow and industrial bromide input, *Water Resour. Res.*, *40*, W01602, doi:10.1029/2003WR002458.

Salehin, M., A. I. Packman, and M. Paradis (2004), Hyporheic exchange with heterogeneous streambeds: Laboratory experiments and modeling, *Water Resour. Res.*, *40*, W11504, doi:10.1029/2003WR002567

Sawyer, A. H., and M. B. Cardenas (2009), Hyporheic flow and residence time distributions in heterogeneous cross-bedded sediment, *Water Resour. Res.*, *45*, W08406, doi:10.1029/2008WR007632.

Sidle, R. C., and Y. Onda (2004), Hydrogeomorphology: Overview of an emerging science, *Hydrol. Processes*, *18*(4), 597–602, doi:10.1002/hyp.1360.

Sivapalan, M. (2003), Process complexity at hillslope scale, process simplicity at the watershed scale: Is there a connection?, *Hydrol. Processes*, *17*(5), 1037–1041, doi:10.1002/hyp.5109.

Stanford, J. A., and J. V Ward (1993), An ecosystem perspective of alluvial rivers: Connectivity and the hyporheic corridor, *J. N. Am. Benthol. Soc.*, *12*(1), 48–60.

Storey, R. G., K. W. F. Howard, and D. D. Williams (2003), Factors controlling riffle-scale hyporheic exchange flows and their seasonal changes in a gaining stream: A three-dimensional groundwater flow model, *Water Resour. Res.*, *39*(2), 1034, doi:10.1029/2002WR001367.

Swanson, F. J., and M. E. James (1975), Geology and geomorphology of the H.J. Andrews experimental Forest, western Cascades, Oregon, *Northwest Science*, *49*(1), 1–11.

Swanson, F. J., and J. A. Jones (2002), Geomorphology and hydrology of the H.J. Andrews Experimental Forest, Blue River, Oregon, Field Guide to Geologic Processes in Cascadia, Oregon Department of Geology and Mineral Industries Special Paper 36, 289–314.

Trauth, N., C. Schmidt, U. Maier, M. Vieweg, and J. H. Fleckenstein (2013), Coupled 3-D stream flow and hyporheic flow model under varying stream and ambient groundwater flow conditions in a pool-riffle system, *Water Resour. Res.*, *49*, 5834–5850, doi:10.1002/wrcr.20442.

Van Genuchten, M. T., and P. J. Wierenga (1976), Mass transfer studies in sorbing porous media I. Analytical solutions, *Soil Sci. Soc. Am. J.*, *40*(4), 473–480.

Valett, H. M., J. A. Morrice, C. N. Dahm, and M. E. Campana (1996), Parent lithology, surface-groundwater exchange, and nitrate retention in headwater streams, *Limnol. Oceanogr.*, *41*(2), 333–345.

Vaux, W. G. (1968), Intragravel flow and interchange of water in a streambed, *Fish. Bull.*, *66*(3), 479–489.

Vervier, P., J. Gibert, P. Marmonier, S. Journal, N. American, B. Society, N. Mar, and M. J. Dole-Olivier (1992), A perspective on the permeability of the surface freshwater-groundwater ecotone, *J. N. Am. Benthol. Soc.*, *11*(1), 93–102.

Voltz, T., M. N. Gooseff, A. S. Ward, K. Singha, M. Fitzgerald, and T. Wagener (2013), Riparian hydraulic gradient and stream-groundwater exchange dynamics in steep headwater valleys, *J. Geophys. Res. Earth Surf.*, *118*, 953–969, doi:10.1002/jgrf.20074.

Wagener, T., M. Sivapalan, P. Troch, and R. Woods (2007), Catchment Classification and Hydrologic Similarity, *Geogr. Compass*, *1*(4), 901–931, doi:10.1111/j.1749-8198.2007.00039.x.

Ward, A. S., M. N. Gooseff, and P. A. Johnson (2011), How can subsurface modifications to hydraulic conductivity be designed as stream restoration structures? Analysis of Vaux's conceptual models to enhance hyporheic exchange, *Water Resour. Res.*, *47*, W08512, doi:10.1029/2010wr010028.

Ward, A. S., M. Fitzgerald, M. N. Gooseff, T. J. Voltz, A. M. Binley, and K. Singha (2012), Hydrologic and geomorphic controls on hyporheic exchange during base flow recession in a headwater mountain stream, *Water Resour. Res.*, *48*, W04513, doi:10.1029/2011WR011461.

Ward, A. S., M. N. Gooseff, T. J. Voltz, M. Fitzgerald, K. Singha, and J. P. Zarnetske (2013a), How does rapidly changing discharge during storm events affect transient storage and channel water balance in a headwater mountain stream?, *Water Resour. Res.*, *49*, 5473–5486, doi:10.1002/wrcr.20434.

Ward, A. S., R. A. Payn, M. N. Gooseff, B. L. McGlynn, K. E. Bencala, C. a. Kelleher, S. M. Wondzell, and T. Wagener (2013b), Variations in surface water-ground water interactions along a headwater mountain stream: Comparisons between transient storage and water balance analyses, *Water Resour. Res.*, *49*, 3359–3374, doi:10.1002/wrcr.20148.

Ward, A. S., M. N. Gooseff, M. Fitzgerald, T. J. Voltz, and K. Singha (2014), Spatially distributed characterization of hyporheic solute transport during baseflow recession in a headwater mountain stream using electrical geophysical imaging, *J. Hydrol.*, *517*, 362–377, doi:10.1016/j.jhydrol.2014.05.036.

White, D. S., S. Journal, N. American, and B. Society (1993), Perspectives on defining and delineating hyporheic zones, *J. N. Am. Benthol. Soc.*, *12*(1), 61–69.

Wondzell, S. M. (2006), Effect of morphology and discharge on hyporheic exchange flows in two small streams in the Cascade Mountains of Oregon, USA, *Hydrol. Processes*, *20*(2), 267–287.

Wondzell, S. M. (2011), The role of the hyporheic zone across stream networks, *Hydrol. Processes*, *25*(22), 3525–3532, doi:10.1002/hyp.8119.

Wondzell, S. M., and F. J. Swanson (1996), Seasonal and storm dynamics of the hyporheic zone of a 4 th-order mountain stream. 2: Nitrogen cycling, *J. N. Am. Benthol. Soc.*, *15*(1), 3–19,

Wondzell, S. M., M. N. Gooseff, and B. L. McGlynn (2007), Flow velocity and the hydrologic behavior of streams during baseflow, *Geophys. Res. Lett.*, *34*, L24404, doi:10.1029/2007GL031256.

Wondzell, S. M., J. LaNier, and R. Haggerty (2009), Evaluation of alternative groundwater flow models for simulating hyporheic exchange in a small mountain stream, *J. Hydrol.*, *364*(1-2), 142–151.

Wondzell, S. M., M. N. Gooseff, and B. L. McGlynn (2010), An analysis of alternative conceptual models relating hyporheic exchange flow to diel fluctuations in discharge during baseflow recession, *Hydrol. Processes*, *24*(6), 686–694.

Wondzell, S. M., M. N. Gooseff, O. Forestry, M. N. Gooseff, and O. Forestry (2013), Geomorphic controls on hyporheic exchange across scales: Watersheds to particles, in *Treatise on Geomorphology*, vol. 9, edited by J. Schroder and E. Wohl, pp. 203–218, Academic, San Diego, Calif.

Worman, A., A. I. Packman, and K. Jonsson (2002), Effect of flow-induced exchange in hyporheic zones on longitudinal transport of solutes in streams and rivers, *Water Resour. Res.*, *38*(1), 1001, doi:10.1029/2001WR000769.

Wright, K. K., Baxter, and J. L. Li (2005), Restricted hyporheic exchange in an alluvial river system: Implications for theory and management, *J. N. Am. Benthol. Soc.*, *24*(3), 447–460.

Zarnetske, J. P., M. N. Gooseff, T. R. Brosten, J. H. Bradford, J. P. McNamara, and W. B. Bowden (2007), Transient storage as a function of geomorphology, discharge, and permafrost active layer conditions in Arctic tundra streams, *Water Resour. Res.*, *43*, W07410, doi:10.1029/2005WR004816.